Transactions on Energy Systems and Engineering Applications

Article

Numerical Study in Effect of Thermal Slip on Two Fluid Flow in a Vertical Channel

Vasavi Cheruku[1] and B. Ravindra Reddy[2]

[1] Department of Mathematics, Sreyas Institute of Engineering and Technology, Hyderabad, Telangana, India.
[2] Department of Mathematics, JNTUH College of Engineering Hyderabad, Hyderabad, 500085, India.
* Correspondence: vaasaviemaths@gmail.com; rbollareddy@gmail.com

Received: 16 May 2023; Accepted: 5 July 2023; Published: 17 July 2023

Abstract: The present study investigates the effect of thermal slip on an immiscible flow of micropolar and viscous fluids in a vertical channel. The left boundary is subjected to thermal slip with appropriate boundary and interface conditions, resulting in a linked system of nonlinear partial differential equations. The ND Solve technique in Mathematica software is used to implement the Runge-Kutta method of the sixth order. The velocity, temperature, and concentration equations are then calculated. The mass, heat, and velocity transmission rates at the boundaries were recorded for all the variations in the governing parameters. In addition, the impact of relevant parameters on various physical properties of micropolar and viscous fluids is analyzed through graphical means. The results are then discussed in detail. Thermal slip, Grashof number, molecular number, magnetic parameter, and Reynolds number are crucial factors that significantly affect heat and mass transfer in fluid flow. The effect of the increased thermal slip is noted to result in a decrease in both the velocity profile and temperature. It was also observed that higher values of Grashof and molecular Grashof numbers led to increased velocity and angular velocity.

1. Introduction

Currently, many researchers are interested in methodologies involving slip conditions, and there is a high demand for thermal systems that depend on industry. Subsequently, other scholars have applied the partial-slip boundary constraint idea with variable fluids and complicated geometries. The goal of this research, inspired by Zheng et al. [1] the combined effects of partial slip and temperature jump on the free convective flow of heat-producing and absorbing fluid through micro-channels were to be investigated. Ramesh et al. [2] provided the torque stress fluid flow survey with pumping strategy under the input of MHD and porous medium. Haddad et al. [3] [4] provide more information on velocity slips and temperature jumps. Bs Babu et al. [5] studies the effects of non-uniform fluid viscosity and thermal conductivity on the MHD flow and heat transfer of a fluid in a vertical channel with a heat source by taking thermal slip.

How to cite this article: Cheruku, Vasavi;Reddy,B. Ravindra. Numerical Study in Effect of Thermal Slip on Two Fluid Flow in a Vertical Channel. *Transactions on Energy Systems and Engineering Applications*, 4(2): 517, 2023. DOI:10.32397/tesea.vol4.n2.517

Symbol	Description	Unit
U_1, U_2	Velocities in Region 1 and Region 2	m/s
U_0	Average Velocity	m/s
T_1, T_2	Temperatures of the plate at $y = -h_1$ and $y = -h_2$	K
T_0	Average temperature	K
k_1, k_2	Thermal conductivity in Region 1 and Region 2	m^2/s
g	Acceleration due to gravity	m/s^2
H_0	Magnetic Field Intensity	Tesla
st_1, st_2	Shear stress at $y = -1$ and $y = 1$	kg/ms^2
ρ_1, ρ_2	Density of fluid in Region 1 and Region 2	kg/m^3
β_1, β_2	Coefficient of Thermal expansion in Region 1 and Region 2	K^{-1}
μ_1, μ_2	Viscosity of fluid in Region 1, Region 2	kg/ms
σ	Electrical conductivity	S/m
μ_e	Magnetic Field Permeability	N/A^2
K	Vertex viscosity	m^2/s

Table 1. Description of symbols and units.

Sharma et al. [6] examined the MHD slip flow and heat transfer of a viscous incompressible fluid across a flat exponentially nonconducting stretched porous sheet using MATLAB software. Kemparaju et al. [7] examined heat transfer in MHD Newtonian fluid flow across a stretched sheet in the presence of velocity and thermal slip. Hayat et al. [8] investigated MHD flow and heat transfer parameters for boundary layer flow across a permeable stretched sheet with thermal slip. Lodhi and Ramesh et al. [9] investigated MHD Jeffrey fluid flow in the presence of electroosmosis, slip effects, and a modified Darcy's equation. Suresh Babu et al. [10] [11] studied the Heat and mass transport fluid flow in a vertical channel using FEM. Aziz [12] studied hydrodynamic and thermal slip flow boundary layers over a flat plate with constant heat flux boundary conditions. He concluded that as the slip parameter increases, the slip velocity increases, and the wall shear stress decreases. Manjunatha et al. [13] [14] used the partial slip boundary constraints idea with various fluids and complicated geometries. The heat equation and Stokes equations with slip boundary conditions have been taken into consideration by Djoko et al. [15].

Magneto hydrodynamics research has gained prominence due to its widespread application in accelerators, liquid metal cooling systems, geothermal power generation, compressed beds for the chemical industry, MHD power generators, plasma studies, boundary layer control in aerodynamics, and other fields. Asadulla et al. [16] studied the hydromagnetic flow in irregularly shaped channels. Hosseini et al. [17] used the difference transformation approach to study flux through non-uniform channels under the influence of a magnetic field. Hatami et al. [18] studied how a magnetic field affects the two-phase flow between two parallel plates. Kamel et al. [19] studied the transport of a liquid-particle suspension in a flexible-walled tube by considering sliding effects along the wall. Eldesoky et al. [20] carried out an analytical investigation of particle suspension in a tube with wavy walls. Chalgeri et al. [21] conducted an experimental study of two-phase flows in a channel with rectangular walls. Chamka et al. [22] analyzed the suspension flow of hydromagnetic particles along a channel analytically. The thermal effects of diffusion and diffusion on convective heat and mass transfer along a vertical channel filled with viscous and micropolar fluids are described by Suresh Babu et al. [23]. Bhargava et al. [24] discovered that the magneto hydrodynamic micropolar fluid free displacement between two vertical porous plates decreases with increasing Hartmann number.

Two-phase flow is applied by a variety of scientific, engineering, and technological fields. Examples include gas-liquid flow in boilers, aerosol separation in spray treatment and oil and gas production

examples, gas-liquid flow in boilers, aerosol separation in spray treatment, ocean waves, ink jets, clouds, fog, groundwater movement, pest control and oil and gas production all benefit greatly from two-phase flows. The two-phase flows in different geometries have been studied by several scholars [25] [26] [27]. Heat transfer in communication channels with non-parallel walls was studied by Sparrow et al. [28] who found that converging and diverging channels transfer heat at a rate significantly higher than channels with parallel walls.

Mathematical software programmes are frequently used to solve complex challenges in today's society. For solving complex differential equations (DEs), Mathematica is a significant computer algebra system to employ differential equations. In mathematics, ND Solve refers to the solutions as interpolating function objects. NDSolve currently calculates differential-equations solution using the numerical technique of lines. NDSolve has a lot of built-in commands, including shooting and Runge-Kutta methods. As a result, several authors have employed the computational tool Mathematica/MATLAB in a variety of complex situations. For instance, Khan et al. [29] MAT LAB results for the motion of nano liquid across spinning discs under the magneto hydrodynamic effects are available. Using shooting and Runge-Kutta techniques, Kumar et al. [30] investigated the MHD radioactive flow of Casson liquid through an exponentially stretched region.

Based on the above requirements and the significance of thermal slip, the current study concentrates on the numerical solution in an immiscible flow including both micropolar and viscous liquids in a vertical channel with the impact of thermal slip.

2. MATHEMATICAL FORMULATION

Consider two isothermal parallel plates, divided into two regions: Region-1 at $y = -h_1$ filled with micropolar fluid and Region-2 at $y = h_2$ filled with viscous fluid. These two zones are kept at T_1 and T_2, respectively. Assuming that the fluid flow has a bouncing effect and is one-dimensional, laminar, immersible, incompressible, and constant transport property. Assuming that the fluid motion is complete and constant. The walls are isothermal with constant concentration and satisfy relation $T_1 > T_2, C_1 > C_2$. Figure 1 illustrates the Schematic diagram.

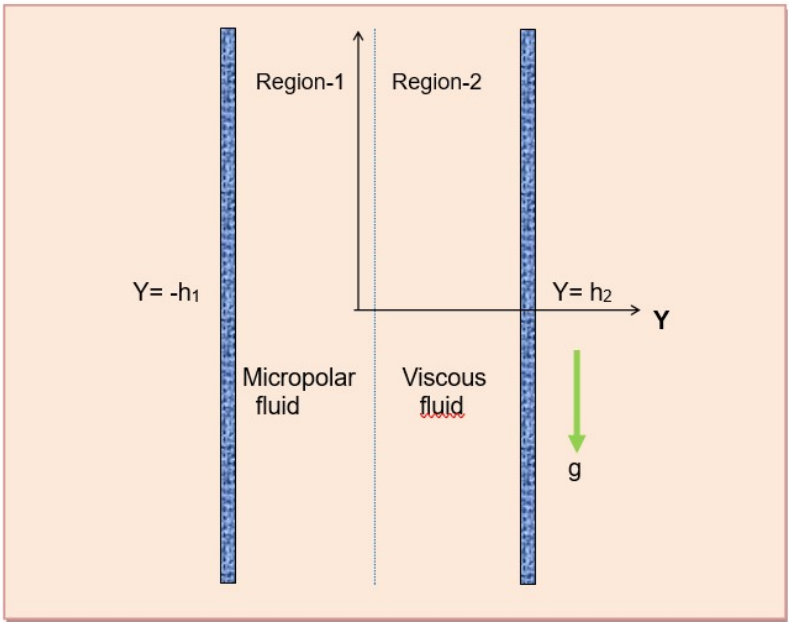

Figure 1. Schematic diagram

The following equations result from the governing equations under the presumptions mentioned above, parameters used are described in Table 1.

Region-1

$$\frac{\partial U_1}{\partial Y} = 0, \tag{1}$$

$$\rho_1 = \rho_0[1 - \beta_{1T}(T_1 - T_0) - \beta_{1C}(C_1 - C_0)], \tag{2}$$

$$\frac{\mu_1 + K}{\rho_1}\frac{\partial^2 U_1}{\partial Y^2} + \frac{K}{\rho_1}\frac{\partial n}{\partial Y} + g\beta_{1T}\left(T_1 - T_0\right) + g\beta_{1C}\left(C_1 - C_0\right) - \frac{\sigma {B_0}^2 U_1}{\rho_1} = 0, \tag{3}$$

$$\gamma\frac{\partial^2 n}{\partial Y^2} - K\left[2n + \frac{\partial U_1}{\partial Y}\right] = 0, \tag{4}$$

$$\text{where } \gamma = \left(\mu_1 + \frac{K}{2}\right) j,$$

$$\frac{k_1}{\rho_1 C_p}\frac{\partial^2 T_1}{\partial Y^2} + \frac{1}{\rho_1 C_p}\left[\mu_1\left(\frac{\partial U_1}{\partial Y}\right)^2 + \frac{\rho_1 D_1 K_{T1}}{C_{S1}}\frac{\partial^2 C_1}{\partial Y^2}\right] = 0, \tag{5}$$

$$D_1\frac{\partial^2 C_1}{\partial Y^2} + \frac{D_1 K_{T1}}{T_M}\frac{\partial^2 T_1}{\partial Y^2} = 0. \tag{6}$$

Region-2

$$\frac{\partial U_2}{\partial Y} = 0, \tag{7}$$

$$\rho_2 = \rho_0[1 - \beta_{2T}(T_2 - T_0) - \beta_{2C}(C_2 - C_0)], \tag{8}$$

$$\frac{\mu_2}{\rho_2}\frac{\partial^2 U_2}{\partial Y^2} + g\beta_{2T}\left(T_2 - T_0\right) + g\beta_{2C}\left(C_2 - C_0\right) - \frac{\sigma {B_0}^2 U_2}{\rho_2} = 0, \tag{9}$$

$$\frac{k_2}{\rho_2 C_p}\frac{\partial^2 T_2}{\partial Y^2} + \frac{1}{\rho_2 C_p}\left[\mu_2\left(\frac{\partial U_2}{\partial Y}\right)^2 + \frac{\rho_2 D_2 K_{T2}}{C_{S2}}\frac{\partial^2 C_2}{\partial Y^2}\right] = 0, \tag{10}$$

$$D_2\frac{\partial^2 C_2}{\partial Y^2} + \frac{D_2 K_{T2}}{T_M}\frac{\partial^2 T_2}{\partial Y^2} = 0. \tag{11}$$

The following boundary and interface conditions when attempting to solve the system of equations Eq. (1) to (11) are considered respectively as,

$$U_1 = 0 \quad \text{at } Y = -h_1 \tag{12}$$

$$U_2 = 0 \quad \text{at } Y = h_2, \quad U_1(0) = U_2(0) \tag{13}$$

$$T_1 = T_0 + B\frac{\partial T_1}{\partial Y} \quad \text{at } Y = -h_1 \tag{14}$$

$$T = T_2 \quad \text{at } Y = h_2 \tag{15}$$

$$T_1(0) = T_2(0) \tag{16}$$

$$C = C_1 \quad \text{at } Y = -h_1 \tag{17}$$

$$C = C_2 \quad \text{at } Y = h_2 \tag{18}$$

$$C_1(0) = C_2(0) \tag{19}$$

$$n = 0 \quad \text{at } Y = -h_1 \tag{20}$$

$$(\mu_1 + K)\frac{\partial U_1}{\partial Y} + Kn = \mu_2 \frac{\partial U_2}{\partial Y} \quad \text{at } Y = 0 \tag{21}$$

$$\frac{\partial n}{\partial Y} = 0 \quad \text{at } Y = 0 \tag{22}$$

$$k_1 \frac{\partial T_1}{\partial Y} = k_2 \frac{\partial T_2}{\partial Y} \quad \text{at } Y = 0 \tag{23}$$

$$D_1 \frac{\partial C_1}{\partial Y} = D_2 \frac{\partial C_2}{\partial Y} \quad \text{at } Y = 0 \tag{24}$$

The following non-dimensional variables and also the variables described in Table 2 are utilized to get the system of equations Eq. (1) through Eq. (11) into a dimensionless form,

$$y = \frac{Y}{h_1}(\text{region-1}), y = \frac{Y}{h_2}(\text{region-2}), u_1 = \frac{U_1}{U_0}, u_2 = \frac{U_2}{U_0}, \theta_1 = 1 + \beta\frac{\partial \theta_1}{\partial y} aty = -1, \beta = \frac{B}{h_1}, \tag{25}$$

$$\theta_2 = \frac{T_2 - T_0}{\Delta T}, j = h^2(\text{Characteristic length}), \tag{26}$$

$$C_S = \frac{C_{S1}}{C_{S2}}, K_T = \frac{K_{T1}}{K_{T2}}, D = \frac{D_1}{D_2}, h = \frac{h_1}{h_2}, m = \frac{\mu_1}{\mu_2}, \alpha = \frac{k_1}{k_2}, \rho = \frac{\rho_1}{\rho_2}, b_1 = \frac{\beta_{1T}}{\beta_{2T}}, b_2 = \frac{\beta_{1C}}{\beta_{2C}}, \nu = \frac{\nu_1}{\nu_2}, K' = \frac{K}{\mu_1}. \tag{27}$$

Here are the governing equations dimensionless representations,

Region-1

$$\frac{\partial^2 N}{\partial y^2} - \frac{2K'}{2 + K'}\left(2N + \frac{\partial u_1}{\partial y}\right) = 0, \tag{28}$$

$$\left(1 + K'\right)\frac{\partial^2 u_1}{\partial y^2} + K'\frac{\partial N}{\partial y} + \frac{Gr}{R}\theta_1 + \frac{Gc}{R}c_1 - Mu_1 = 0, \tag{29}$$

$$\frac{1}{PrR}\frac{\partial^2 \theta_1}{\partial y^2} + \frac{Ec}{R}\left(\frac{\partial u_1}{\partial y}\right)^2 + \frac{Du}{R}\frac{\partial^2 c_1}{\partial y^2} = 0, \tag{30}$$

$$\frac{1}{ScR}\frac{\partial^2 c_1}{\partial y^2} + Sr\frac{\partial^2 \theta_1}{\partial y^2} = 0. \tag{31}$$

Region-2

$$\frac{\partial^2 u_2}{\partial y^2} + \frac{m}{b_1 \rho h^2}\frac{Gr}{R}\theta_2 + \frac{m}{b_2 \rho h^2}\frac{Gc}{R}c_2 - \frac{mM}{h^2}u_2 = 0, \tag{32}$$

$$\frac{\rho h}{\alpha}\frac{1}{PrR}\frac{\partial^2\theta_2}{\partial y^2}+\frac{\rho h}{m}\frac{Ec}{R}\left(\frac{\partial u_2}{\partial y}\right)^2+\frac{c_s h}{DK_T}\frac{D_u}{R}\frac{\partial^2 c_2}{\partial y^2}=0, \tag{33}$$

$$\frac{h}{D}\left(\frac{1}{Sc\,R}\right)\frac{\partial^2 c_2}{\partial y^2}+\frac{h}{K_T D}Sr\frac{\partial^2\theta_2}{\partial y^2}=0. \tag{34}$$

The resulting dimensionless boundary and interface conditions are,

$$u_1=0 \text{ at } y=-1, \tag{35}$$

$$u_2=0 \text{ at } y=1, \tag{36}$$

$$u_1(0)=u_2(0), \tag{37}$$

$$\theta_1=1+\beta\frac{\partial\theta}{\partial y} \text{ at } y=-1, \tag{38}$$

$$\theta_2=0 \text{ at } y=1, \tag{39}$$

$$\theta_1(0)=\theta_2(0), \tag{40}$$

$$c_1=1 \text{ at } y=-1, \tag{41}$$

$$c_2=0 \text{ at } y=1, \quad c_1(0)=c_2(0), \tag{42}$$

$$N=0 \text{ at } y=-1, \tag{43}$$

$$\frac{\partial u_1}{\partial y}+\frac{K'}{1+K'}N=\frac{1}{mh(1+K')}\frac{\partial u_2}{\partial y}, \quad \text{at } y=0, \tag{44}$$

$$\frac{\partial N}{\partial y}=0 \text{ at } y=0, \tag{45}$$

$$\frac{\partial\theta_1}{\partial y}=\frac{1}{h\alpha}\frac{\partial\theta_2}{\partial y}, \quad \text{at } y=0, \tag{46}$$

$$\frac{\partial c_1}{\partial y}=\frac{1}{hD}\frac{\partial c_2}{\partial y}, \quad \text{at } y=0. \tag{47}$$

Non-Dimensional number	**Definition**	**Physical meaning**
Thermal Grashof number (Gr)	$Gr=\frac{g\beta_{1T}\Delta T{h_1}^3}{{\nu_1}^2}$	Ratio of Bouncy forces to Friction force
Molecular Grashof number (Gc)	$Gc=\frac{g\beta_{1C}\Delta C{h_1}^3}{{\nu_1}^2}$	Ratio of Bouncy forces to Friction force
Reynolds-number (R)	$R=\frac{U_0 h_1}{v_1}$	Ratio of Inertial forces to viscous forces
Soret-number (Sr)	$Sr=\frac{D_1 K_{T1}\Delta T}{T_M\Delta C U_0 h_1}$	Ratio of kinetic energy to enthalpy
Eckert-number (Ec)	$Ec=\frac{{U_0}^2}{Cp\Delta T}$	Ratio of kinetic energy to enthalpy
Prandtl number (Pr)	$Pr=\frac{\mu_1 Cp}{k_1}$	Ratio of momentum diffusivity and thermal diffusivity
Nusselt Number (Nu)	$Nu=\frac{hd}{k}$	Ratio of convective to conductive heat transfer
Schmidt number (Sc)	$Sc=\frac{v_1}{D_1}$	Ratio of Viscous diffusion rate to molecular diffusion rate
Dufour number (Du)	$Du=\frac{D_1 K_{T1}\Delta C}{C_P C_{S1}\nu_1\Delta T}$	Ratio of diffusion gradient to thermal energy rate

Table 2. Non-Dimensional numbers.

3. SOLUTION OF THE PROBLEM

Using the 6^{th} order Runge-Kutta approach, a system of nonlinear equations is solved numerically. Numerical calculations using the thermal slip effect were performed for several relevant parameter values. The parameters are thermal Grashof-number (Gr), Molecular Grashof-number (Gc), Reynolds-number (R), Magnetic-field parameters (M), Material-parameters (K'), Dufour-number (Du), Schmidt-number (Sc), Soret-number (Sr) and Eckert-number (Ec). The effects of governing parameters and slip parameters on the dimensionless parameter's velocity, temperature, and concentration are generated in graphic form. The rate of transmission along both walls is studied using the following equations,

$$st_1 = \left[\frac{\partial u_1}{\partial y}\right]_{y=-1}, \quad st_2 = \left[\frac{\partial u_2}{\partial y}\right]_{y=1}, \quad Nu_1 = \left[\frac{\partial \theta_1}{\partial y}\right]_{y=-1}, \quad Nu_2 = \left[\frac{\partial \theta_2}{\partial y}\right]_{y=1}, \tag{48}$$

$$Sh_1 = \left[\frac{\partial c_1}{\partial y}\right]_{y=-1}, \quad Sh_2 = \left[\frac{\partial c_2}{\partial y}\right]_{y=1}, \tag{49}$$

4. RESULTS AND DISCUSSIONS

The system of nonlinear partial differential equations, along with the corresponding boundary conditions, was solved using the Runge-Kutta 6^{th} order method with the Mathematica ND Solve. Significant computational analyses have been carried out to elucidate the impact of important physical parameters, such as the Gr, Gc, k, R and Thermal slip parameter (β) on physical quantities, specifically velocity, angular velocity, temperature, diffusion.

Figure 2 to Figure 6 shows the effect of Gr and Gc, k, R and β on velocity profiles. Figures 2,3 describes that as Gr, Gc increases, the velocity also increases significantly this is because the fluid velocity increases due to amplification of thermal and species buoyancy forces. the results are well mapped with Suresh Babu et al. [31] [32]. Figure 4 illustrates, as the permeability parameter K' increases, it can be seen that the velocity profile decreases. The results are in line with Bilal et al [33]. However, the velocity decreased as the parameter R increased, as shown in Figure 5. The effect of thermal slip parameter is depicted in Figure 6, from the graph the nature is very clear that the velocity is inversely proportional to slip parameter also the nature is parabolic and symmetric about interface. This is because of the imposition of boundary values on the system owing to the effect of temperature variation on the boundary. Figure 7 illustrate the effect of magnetic parameter M on velocity. Velocity decreases with an increase of M, because the application of a transverse magnetic field acts as a drag force (Lorentz force) acting in the opposite direction of fluid motion and resisting flow, thereby slowing the fluid's velocity.

Figure 8 to Figure 13 Illustrates the effect of Gr and Gc, K', R, β and M on angular velocity. Angular velocity increases with an increase of Gr and Gc this is because of the enhancement of thermal and species buoyancy forces. Presence of viscous forces decreases angular velocity as there is an increment in the parameters R, K', β substantially. The results are similar to the Gbadeyan et al. [34]

Figure 14 to Figure 17 illustrates the influence of Thermal slip (β) Soret number (Sr), Schmidt number (Sc), Reynolds number (R) on temperature. Figure 14 describes Thermal slip parameter varies $\beta = 0.2, 0.5, 1, 1.5, 2$ which leads to temperature decrement as slip is increases, the thermal slip essentially slows down fluid velocity, which ultimately results in a reduction in net molecular mobility. The thermal slip parameter can regulate the temperature inside the flow, which leads to lesser molecular movement results a drop in temperature. Figure 15 depicts the effect of Sr on temperature and it is observed that as Sr increases temperature is reduced this is because the increase of diffusion among fluid particles. The results are similar to the Ganesh et al. [35].

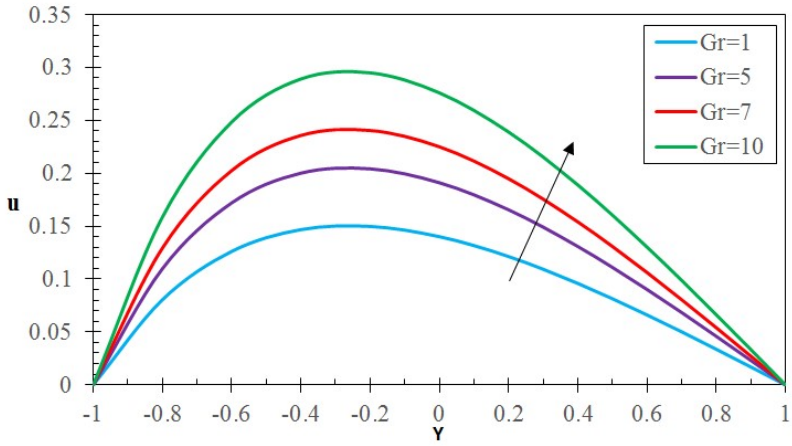

Figure 2. Variations of Velocity with Gr

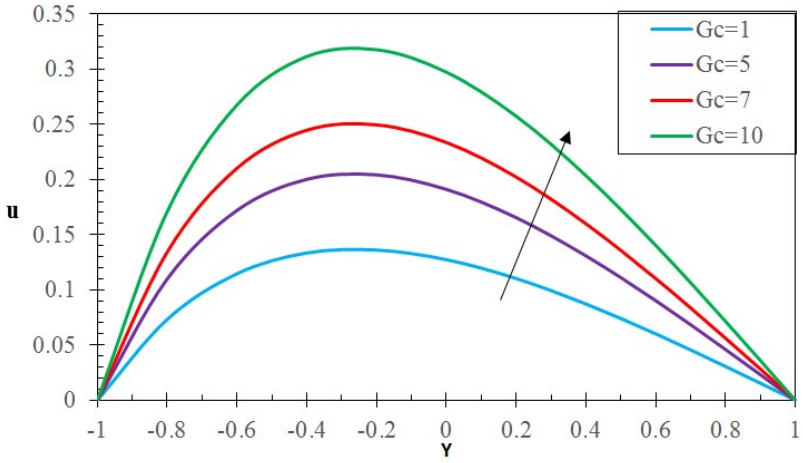

Figure 3. Variations of Velocity with Gc

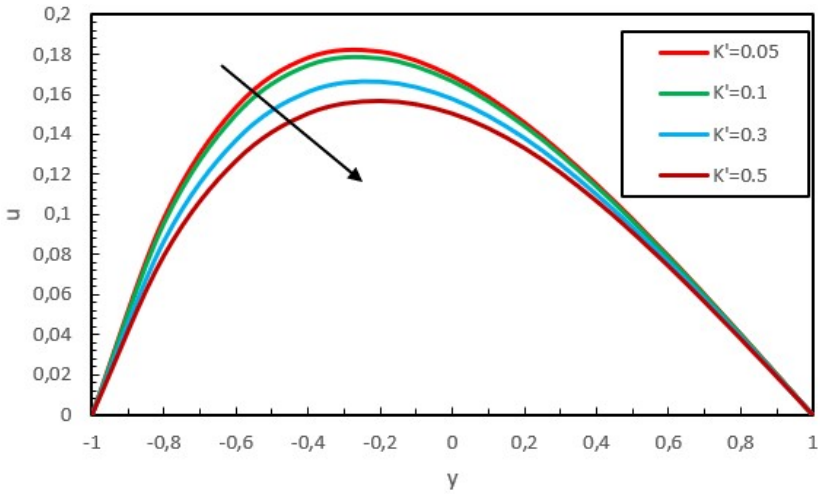

Figure 4. Variations of Velocity with K'

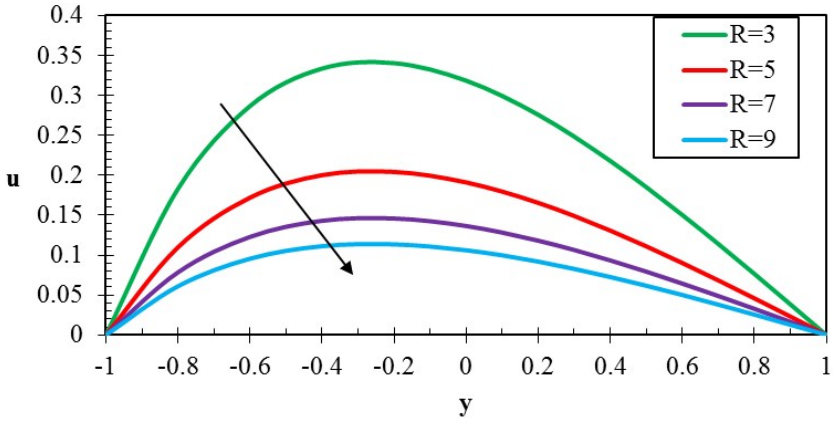

Figure 5. Variations of Velocity with R

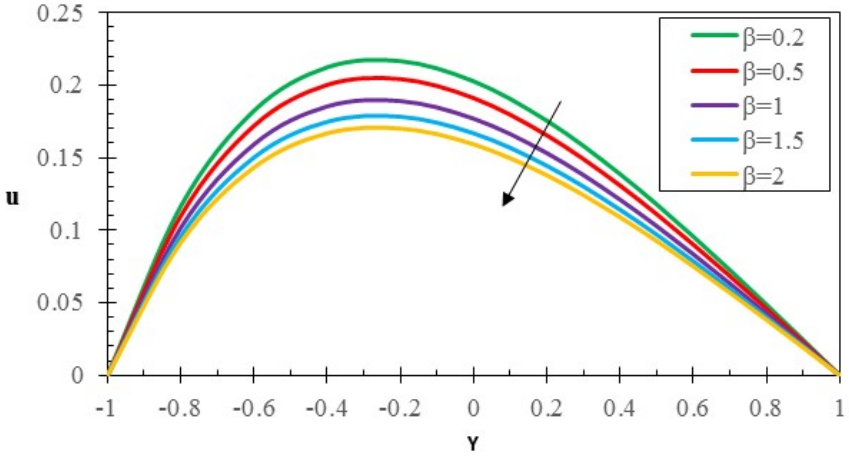

Figure 6. Variation of Velocity with β

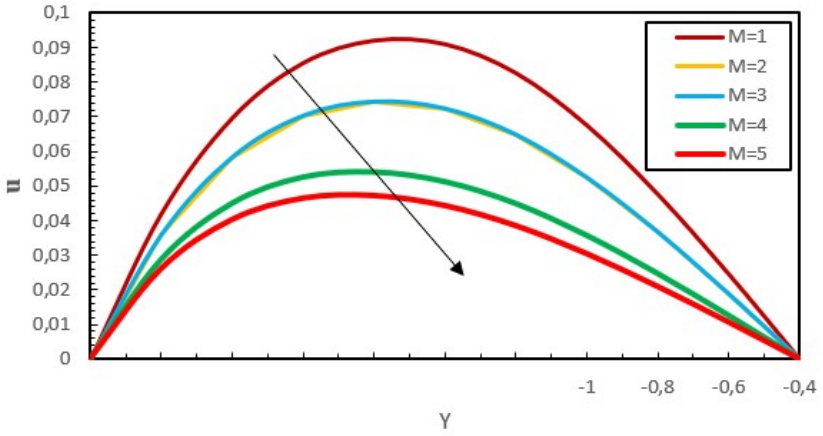

Figure 7. Variation of velocity with M

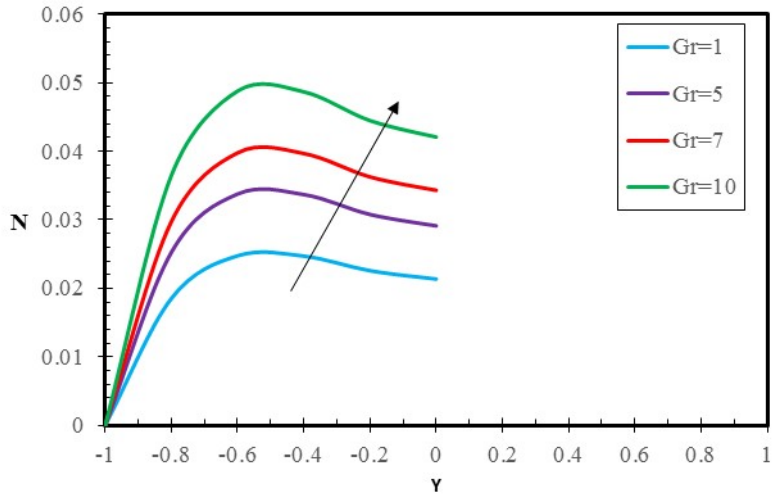

Figure 8. Variations of Angular Velocity with Gr

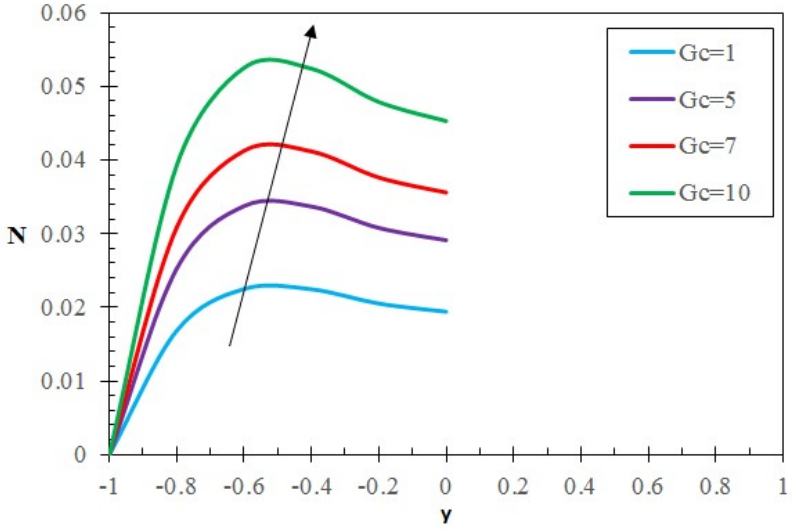

Figure 9. Variations of Agular Velocity with Gc

Figure 16 describes the effect of Sc on temperature, here kinematic viscosity is dominated by mass diffusivity which leads to the temperature decrease with an increase of Schmidt number. As the Reynolds number is dependent of inertial forces and viscous forces, due to the increase of inertial forces in the fluid of the channel lead to diminishing of viscous forces as a result the temperature is lowered as R is increasing from 0.22 to 2.02 as shown in Figure 17.

Figure 18(a) to 18(d) displays the validation outcomes pertaining to the velocity, angular velocity, temperature, and concentration of the fluid flow in the current study, in comparison to the findings of Suresh et al. [31], it is noteworthy that the present results are closely with those results.

Table 3 shows the computed Shear stress, Nusselt number, and Sherwood number together with all possible impact on the governing parameters. Which are obtained when the other parameters are fixed as $Gr = 5, Gc = 5, R = 3, M = 3, K' = 0.1, Du = 0.08, Sr = 0.1, Sc = 0.66, Ec = 0.001$. The Table 3 demonstrates how an increase in absolute Shear stress, which improves shearing outcomes, occurs

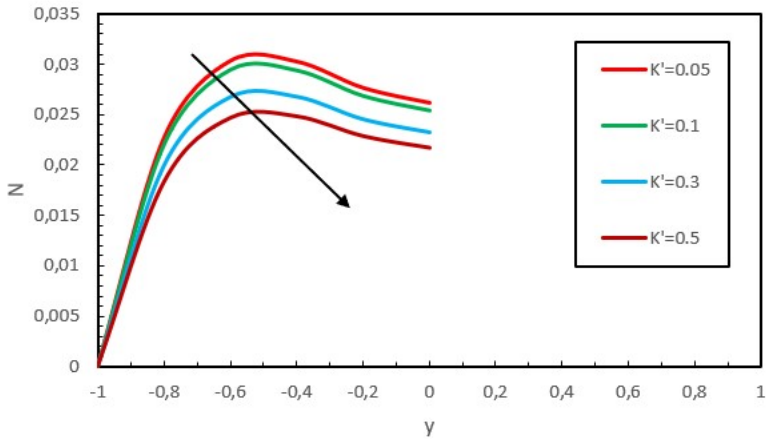

Figure 10. Variation of Angular Velocity with K'

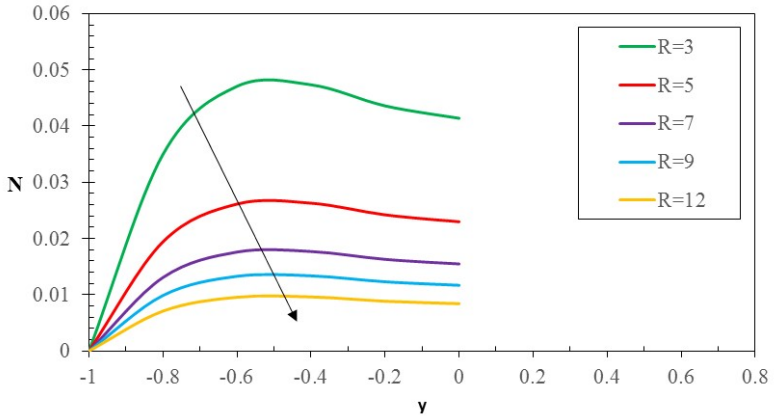

Figure 11. Variation of Angular velocity with R

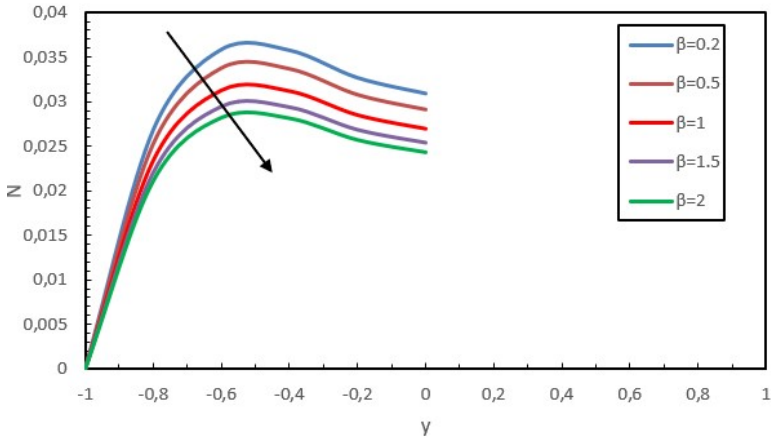

Figure 12. Variation of Angular Velocity with β

when buoyant forces rise close to the boundaries. With an increase in the thermal slip, Reynolds number, Magnetic field parameter, Material parameter, Soret number, and Schmidt number, the Shearing stress at the boundary reduces.

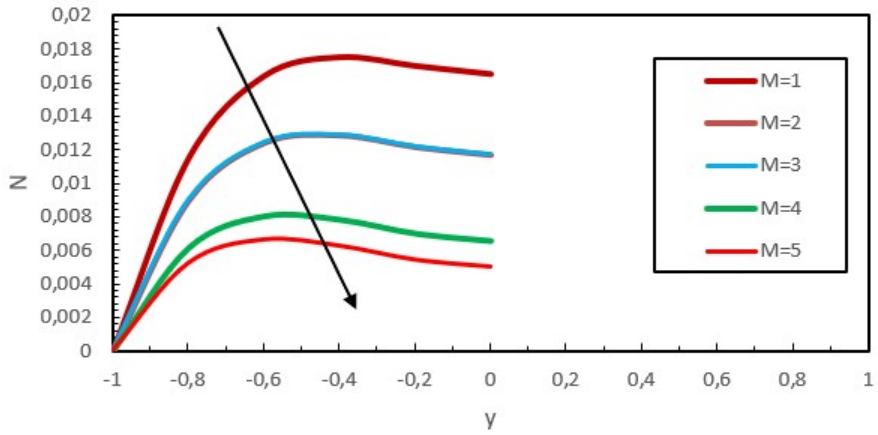

Figure 13. Variation of Angular velocity with M

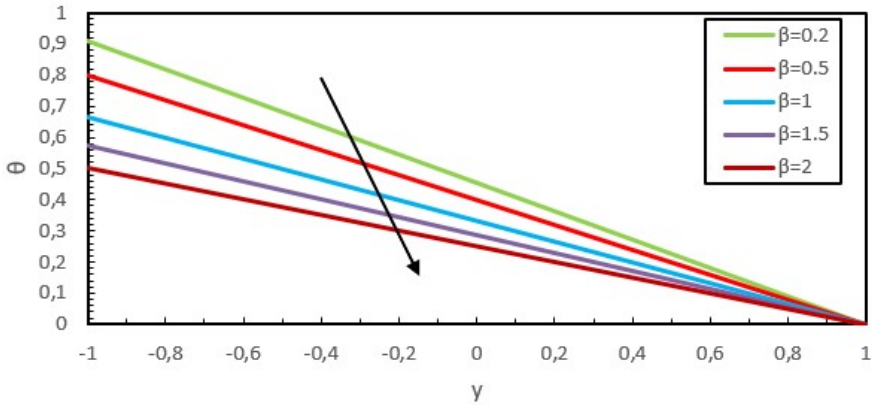

Figure 14. Variation of Temperature with β

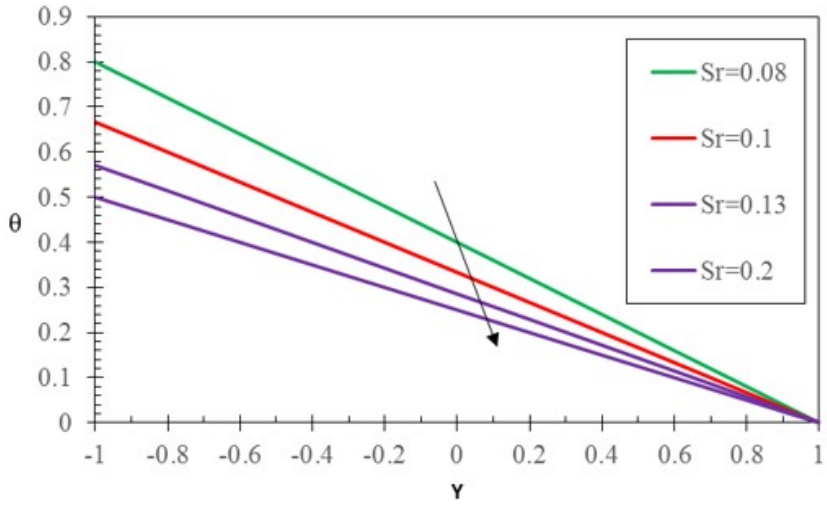

Figure 15. Variation of Temperature with Sr

For the parameters *Gr*, *Gc*, *Sr*, and *Sc*, the Nusselt number, or rate of heat transfer, falls near to one boundary and rises at the other. The rate of heat transmission is significantly affected by variations in the

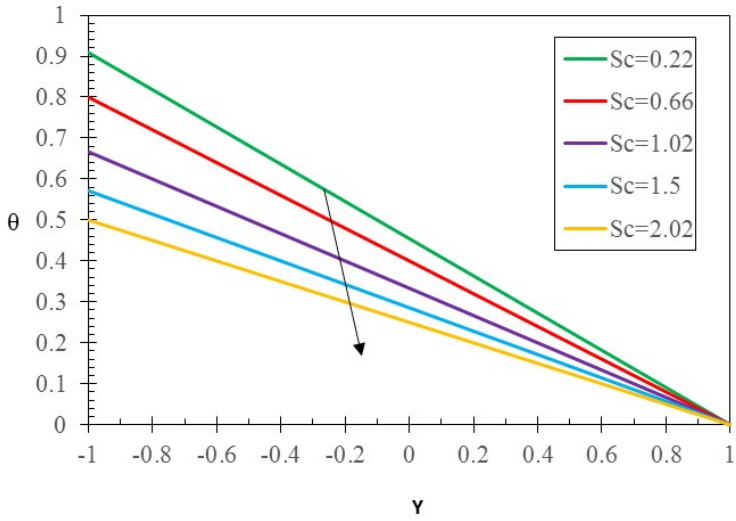

Figure 16. Variation of Temperature with Sc

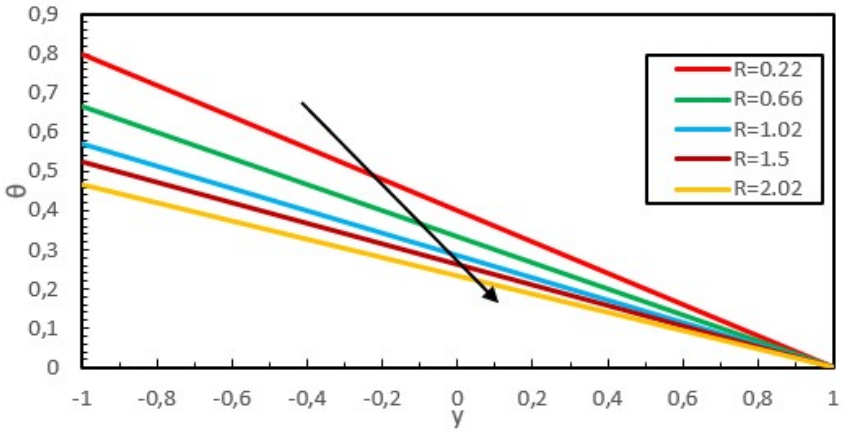

Figure 17. Variation of Temperature with R

Reynolds Number. The increased inertial forces boost the right plate's heat transfer rate while ruining the left plate. The effect is reversed for the values M and k. two borders, the heat transfer rate is reduced due to the thermal slip parameter. The relationship between the Nusselt number and the diffusion parameters Du and Sr shows that as Dufour increases, heat transfer to the left plate increases and decreases to the right plate. For Sr, Sc it is completely opposite.

For the parameters Gr, Gc, R, Sr, Sc, and Ec, the Sherwood number, which measures the rate of mass transfer, increases near one limit and decreases at the other limit. For the other parameters M, K' and Du the mass transfer decreases near the left limit and increases at the right limit, and for the slip parameter the mass transfer rate is reduced at both limits.

5. Conclusions

The present paper analyses the steady MHD convective immiscible two fluid flow of micropolar and viscous fluids along a vertical channel with the effect of thermal slip. Numerical calculations are carried out for various values of nondimensional parameters of the problem with the help of Runge-kutta 6th order

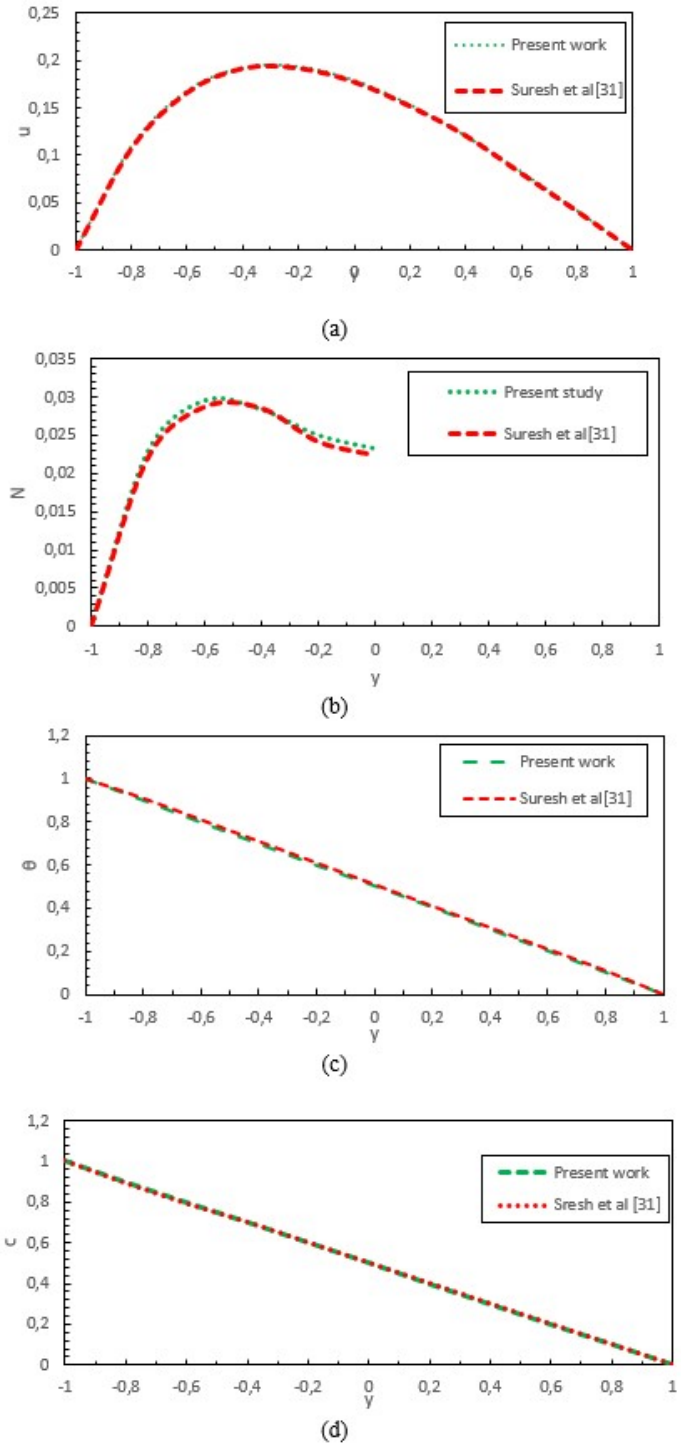

Figure 18. (a) Validation of velocity profiles,(b) Validation of Angular velocity profiles,(c) Validation of Temperature profiles, (d) Validation of Diffusion profiles.

Gr	**St1**	**St2**	**Nu1**	**Nu2**	**Sh1**	**Sh2**
2	0.511333	-0.16945	-0.399969	-0.40002	-0.50001	-0.5
5	0.697282	-0.23108	-0.399943	-0.40004	-0.50002	-0.49999
7	0.821255	-0.27216	-0.399921	-0.40006	-0.50003	-0.49999
10	1.00723	-0.3338	-0.399881	-0.40009	-0.50005	-0.49998
Gc						
2	0.464852	-0.15405	-0.399975	-0.40002	-0.50001	-0.5
5	0.697282	-0.23108	-0.399943	-0.40004	-0.50002	-0.49999
7	0.852237	-0.28243	-0.399915	-0.40006	-0.50004	-0.49999
10	1.08467	-0.35946	-0.399862	-0.4001	-0.50006	-0.49998
R						
2	1.16218	-0.38515	-0.39985	-0.40011	-0.50004	-0.49999
5	0.697282	-0.23108	-0.399943	-0.40004	-0.50002	-0.49999
7	0.498054	-0.16505	-0.399969	-0.40002	-0.50002	-0.49999
9	0.387374	-0.12837	-0.39998	-0.40002	-0.50002	-0.49999
12	0.29053	-0.09628	-0.399988	-0.40001	-0.50001	-0.5
β						
0.2	0.739536	-0.24508	-0.454473	-0.45458	-0.50003	-0.49999
0.54	0.697282	-0.23108	-0.399943	-0.40004	-0.50002	-0.49999
1	0.645637	-0.21396	-0.333293	-0.33338	-0.50002	-0.49999
1.5	0.608747	-0.20174	-0.285683	-0.28576	-0.50002	-0.49999
2	0.581078	-0.19257	-0.249975	-0.25004	-0.50002	-0.49999
K'						
0.05	0.627256	-0.20335	-0.285682	-0.28576	-0.50002	-0.49999
0.1	0.608747	-0.20174	-0.285683	-0.28576	-0.50002	-0.49999
0.3	0.546076	-0.19607	-0.285689	-0.28575	-0.50002	-0.5
0.5	0.497064	-0.19144	-0.285693	-0.28574	-0.50001	-0.5
Sr						
0.05	0.497064	-0.19144	-0.285694	-0.28574	-0.50001	-0.5
0.08	0.497064	-0.19144	-0.285693	-0.28574	-0.50001	-0.5
0.1	0.497064	-0.19144	-0.285693	-0.28574	-0.50001	-0.5
0.13	0.497065	-0.19144	-0.285691	-0.28575	-0.50002	-0.49999
0.2	0.497065	-0.19144	-0.285689	-0.28575	-0.50003	-0.49999
Sc						
0.22	0.497064	-0.19144	-0.285694	-0.28574	-0.5	-0.5
0.66	0.497064	-0.19144	-0.285693	-0.28574	-0.50001	-0.5
1.02	0.497065	-0.19144	-0.285691	-0.28575	-0.50002	-0.49999
1.5	0.497065	-0.19144	-0.285688	-0.28575	-0.50003	-0.49999
2.02	0.497067	-0.19144	-0.285684	-0.28576	-0.50005	-0.49998

Table 3. Numerical values of shear stress, Nusselt number, Sherwood numbers.

method. The influence of all relevant parameters was examined and presented graphically. Some of the most salient findings are as follows:

- The fluid velocity profile raises with higher values of Gr and Gc observed from Figure 2 to Figure 3. However, it follows a decaying function for k and R from Figure 4 to Figure 6.
- The fluid temperature declines with increasing R, Sc, and Sr values which is seen in Figure 12 to Figure 15.
- An increase in the thermal slip effect reduces velocity, angular velocity, and temperature which can be concluded from Figure 6, Figure 11 to Figure 12.
- The Nusselt number, shear stress, and Sherwood number exhibit a decreasing trend with an increase in the slip parameter β it can observe from Table 3.

Acknowledgments

Authors acknowledge the reviewers for their inputs in improving the quality of the paper.

Funding: This research received no external funding.

Author contributions: Conceptualization, Vasavi Cheruku; Methodology, Vasavi Cheruku ; Software, Vasavi Cheruku, B Ravindra Reddy; Validation, Vasavi Cheruku, B Ravindra Reddy; Writing – Original Draft Preparation, Vasavi Cheruku;Writing – Review & Editing, B Ravindra Reddy.

Disclosure statement: The authors declare no conflict of interest.

References

[1] L. Zheng, J. Niu, X. Zhang, and Y. Gao. Mhd flow and heat transfer over a porous shrinking surface with velocity slip and temperature jump. *Mathematical and Computer Modelling*, 56:133, 2012.

[2] K. Ramesh. Influence of heat and mass transfer on peristaltic flow of a couple stress fluid through porous medium in the presence of inclined magnetic field in an inclined asymmetric channel. *Journal of Molecular Liquids*, 219:256, 2016.

[3] O. Haddad, M. Abuzaid, and M. Al-Nimr. Developing free-convection gas flow in a vertical open-ended microchannel filled with porous media. *Numerical Heat Transfer, Part A: Applications*, 48:693–710, 2005.

[4] O. Haddad, M. Al-Nimr, and J. S. Al-Omary. Forced convection of gaseous slip-flow in porous micro-channels under local thermal non-equilibrium conditions. *Transport in porous media*, 67:453–471, 2007.

[5] G. Kiran Kumar, G. Srinivas, and B. S. Babu. Effects of viscosity, thermal conductivity, and heat source on mhd convective heat transfer in a vertical channel with thermal slip condition. In *Recent Trends in Wave Mechanics and Vibrations*, pages 71–86, 2020.

[6] Sushila Choudhary, P. R. Sharma, and O. D. Makinde. Mhd slip flow and heat transfer over an exponentially stretching permeable sheet embedded in a porous medium with heat source. *Frontiers in Heat and Mass Transfer (FHMT)*, 9(1), 2017.

[7] M. Kemparaju, M. S. Abel, and M. M. Nandeppanavar. Heat transfer in mhd flow over a stretching sheet with velocity and thermal slip condition. *Heat Transfer*, 49, 2015.

[8] T. Hayat, M. Qasim, and S. Mesloub. Mhd flow and heat transfer over permeable stretching sheet with slip conditions. *International Journal for Numerical Methods in Fluids*, 66:963–975, 2011.

[9] R. K. Lodhi and K. Ramesh. Comparative study on electroosmosis modulated flow of mhd viscoelastic fluid in the presence of modified darcy's law. *Chinese Journal of Physics*, 68:106–120, 2020.

[10] G. Srinivas and B. Reddy. Finite element analysis of free convection flow with mhd micropolar and viscous fluids in a vertical channel with dissipative effects. *Journal of Naval Architecture and Marine Engineering*, 8(1):59–69, 2011.

[11] B. Suresh Babu, G. Srinivas, and G. V. P. N. Srikanth. Finite element study of convective heat and mass transfer of two fluids in avertical channel of variable width with soret and dufour effects. In *Numerical Heat Transfer and Fluid Flow*, pages 537–546, 2019.

[12] A. Aziz. Hydrodynamic and thermal slip flow boundary layers over a flat plate with constant heat flux boundary condition. *Communications in Nonlinear Science and Numerical Simulation*, 15:573–580, 2010.

[13] G. Manjunatha, C. Rajashekar, H. Vaidya, K. Prasad, and J. Viharika. Influence of convective conditions on the peristaltic mechanism of power-law fluid through a slippery elastic porous tube with different waveforms. *Multidiscipline Modeling in Materials and Structures*, 2019.

[14] G. Manjunatha et al. Impact of variable transport properties and slip effects on mhd jeffrey fluid flow through channel. *Arabian Journal for Science and Engineering*, 45:417–428, 2020.

[15] J. K. Djoko, V. S. Konlack, and M. Mbehou. Stokes equations under nonlinear slip boundary conditions coupled with the heat equation: A priori error analysis. *Numerical Methods for Partial Differential Equations*, 36:86–117, 2020.

[16] M. Asadullah, U. Khan, R. Manzoor, N. Ahmed, and S. T. Mohyud-Din. Mhd flow of a jeffery fluid in converging and diverging channels. *Int. J. Mod. Math. Sci*, 6:92–106, 2013.

[17] R. Hosseini, S. Poozesh, and S. Dinarvand. Mhd flow of an incompressible viscous fluid through convergent or divergent channels in presence of a high magnetic field. *Journal of Applied Mathematics*, 2012, 2012.

[18] M. Hatami, K. Hosseinzadeh, G. Domairry, and M. Behnamfar. Numerical study of mhd two-phase couette flow analysis for fluid-particle suspension between moving parallel plates. *Journal of the Taiwan Institute of Chemical Engineers*, 45:2238–2245, 2014.

[19] Mohammed Saad Kamel, Ferenc Lezsovits, and Ahmed Kadhim Hussein. Experimental studies of flow boiling heat transfer by using nanofluids: a critical recent review. *Journal of Thermal Analysis and Calorimetry*, 138(6):4019–4043, 2019.

[20] I. Eldesoky, S. Abdelsalam, R. Abumandour, M. Kamel, and K. Vafai. Interaction between compressibility and particulate suspension on peristaltically driven flow in planar channel. *Applied Mathematics and Mechanics*, 38:137–154, 2017.

[21] V. S. Chalgeri and J. H. Jeong. Flow patterns of vertically upward and downward air-water two-phase flow in a narrow rectangular channel. *International Journal of Heat and Mass Transfer*, 128:934–953, 2019.

[22] A. J. Chamkha and S. S. Al-Rashidi. Analytical solutions for hydromagnetic natural convection flow of a particulate suspension through isoflux-isothermal channels in the presence of a heat source or sink. *Energy conversion and management*, 51:851–858, 2010.

[23] B. S. Babu, G. Srinivas, and G. Srikanth. Finite element analysis of diffusion effects on convective heat and mass transfer of two fluids in a vertical channel. *International Journal of Automotive & Mechanical Engineering*, 14, 2017.

[24] R. Bhargava, L. Kumar, and H. S. Takhar. Numerical solution of free convection mhd micropolar fluid flow between two parallel porous vertical plates. *International journal of engineering science*, 41(2):123–136, 2003.

[25] A. J. Chamkha. Hydromagnetic two-phase flow in a channel. *International journal of engineering science*, 33:437–446, 1995.

[26] M. Z. Podowski. Multidimensional modeling of two-phase flow and heat transfer. *International Journal of Numerical Methods for Heat & Fluid Flow*, 18(6):763–770, 2008.

[27] S. K. R. Cherlo, S. Kariveti, and S. Pushpavanam. Experimental and numerical investigations of two-phase (liquid-liquid) flow behavior in rectangular microchannels. *Industrial & Engineering Chemistry Research*, 49(2):893–899, 2010.

[28] E. Sparrow and R. Ruiz. Experiments on natural convection in divergent vertical channels and correlation of divergent, convergent, and parallel-channel nusselt numbers. *International journal of heat and mass transfer*, 31(10):2197–2205, 1988.

[29] M. I. Khan et al. Role of dipole interactions in darcy-forchheimer first-order velocity slip nanofluid flow of williamson model with robin conditions. *Applied Nanoscience*, 10:5343–5350, 2020.

[30] K. Anantha Kumar, V. Sugunamma, and N. Sandeep. Effect of thermal radiation on mhd casson fluid flow over an exponentially stretching curved sheet. *Journal of Thermal Analysis and Calorimetry*, 140:2377–2385, 2020.

[31] B. Suresh Babu, G. Srinivas, and G. V. P. N. Srikanth. Finite element study of convectiveheat and mass transfer of two fluids in a vertical channel of variable width with soret and dufour effects. *Numerical Heat Transfer and Fluid Flow*, pages 537–546, 2019.

[32] G. Srinivas and B. R. K. Reddy. Finite element analysis of free convection flow with mhd micropolar and viscous fluids in a vertical channel with dissipative effects. *Journal of Naval Architecture and Marine Engineering*, 8(1):59–69, 2011.

[33] M. Bilal et al. A numerical simulation of electrically conducting micro-channel nanofluid flow with thermal slip effects. *Waves in Random and Complex Media*, pages 1–25, 2022.

[34] J. A. Gbadeyan, E. O. Titiloye, and A. T. Adeosun. Effect of variable thermal conductivity and viscosity on casson nanofluid flow with convective heating and velocity slip. *Heliyon*, 6(1):e03076, 2020.

[35] N. Vishnu Ganesh, Qasem M. Al-Mdallal, and Ali J. Chamkha. A numerical investigation of newtonian fluid flow with buoyancy, thermal slip of order two and entropy generation. *Case Studies in Thermal Engineering*, 13:100376, 2019.